

Studies on Dissimilar Twin-Wire Weld-Deposition for Additive Manufacturing Applications

M. A. Somashekara¹  · S. Suryakumar²

Received: 15 July 2016 / Accepted: 29 December 2016 / Published online: 13 January 2017
© The Indian Institute of Metals - IIM 2017

Abstract Due to its high deposition rate, low cost and simple setup, weld-deposition based additive manufacturing is slowly evolving into a viable alternative for creating meso-scale applications. There is also an increasing demand for creating functionally gradient objects with varying properties. Gas metal arc welding based twin-wire weld-deposition presented here makes it possible to create functionally gradient objects with varying mechanical properties like hardness. This is achieved by using separate filler wires of different composition and controlling the proportion of each wire separately. The current work presents a proof of concept of the twin-wire weld-deposition and also the primary experiments carried out for understanding the effect of weld-deposition process parameter on bead geometry. Two filler wires viz., ER70S-6 and ER110S-G, the former having lower hardness than the latter, were used for the experimentation. The range of process parameter for different combinations of these filler wires was determined and the operating range of the same was identified. Subsequently, the criterion for adapting the twin-wire welding from joining to weld-deposition of a complete layer like thermal steady-state condition, effect of torch direction and effect of overlapping beads have also been studied.

Keywords Welding · Deposition · Additive · Manufacturing · Gradient · Geometry

1 Introduction

Additive manufacturing, also denoted to as layered manufacturing (LM) or rapid prototyping, or 3D printing, has enabled fast, flexible and economically viable products being manufactured according to the information received from CAD data. The last two decades has seen significant research interest being drawn into this area, with the process evolving from prototyping of plastic components to functional metallic parts. The demand from the compressing product development and manufacturing cycles in the industry has also pushed this evolution.

Spencer et al. [1] developed a process named three-dimensional welding for creating metallic components using gas metal arc welding (GMAW) process. Subsequently, many researchers combined the weld-deposition with machining to overcome the problems of accuracy of subsequent layers and oxide layer formation on top of weld-deposition [2]. Karunakaran et al., integrated CNC and weld-deposition to create the near-net shape (using weld-deposition) and final component (using machining) in the same station [3–6]. The study of process planning, operating parameters, accuracy, surface finishing etc., helped in establishing the use of weld-deposition as a viable means of creating homogenous metallic components. However, the potential of weld-deposition to vary the material properties and create functionally gradient materials was not probed.

Welding current, torch speed and wire feed rate were some of the important parameters among the weld-deposition process parameters [5, 7, 8]. As these had an effect on the mechanical properties of the final component, it was important to understand their influence on the process and was studied by various researchers for steel, aluminum etc. Gao et al. [9] noted the effect of the above mentioned

✉ M. A. Somashekara
somashekara.ma@gmail.com

¹ Engineering Product Development (EPD), Singapore
University of Technology and Design (SUTD), Singapore,
Singapore

² Department of Mechanical and Aerospace Engineering, IIT
Hyderabad, Sangareddy, India

process parameters on the weld bead. As expected, increase in the welding current led to higher deposition rate of material and larger cross section area of the weld bead. Increasing the torch speed resulted in a decrease in the cross section area of the bead and became discontinuous after a certain limit. While this study helped in arriving at the optimal value for getting a good weld bead, the possible spectrum of feasible values were not studied. Pal et al. [10] studied effect of torch angle on the welding in both back-hand and forehand welding directions. While this could also potentially be a good means to control the properties, varying the torch orientation would make the kinematic control more complicated, particularly in the context of weld-deposition based AM where the area-filling pattern might vary many times in a given layer. Hence, the present work only uses perpendicular welding condition, where the forward and reverse directions will be same. More parameters like shielding gas, nozzle gap, pulsing parameters were also studied by some researchers [11–15]. However, all of them were related to only single wire welding. Different variants of multiple wire welding like double, tandem, twin-wire and triple-wire welding were also studied by some researchers [16–21]. However, these studies were mainly in the context of using welding as a joining mechanism and not for using it for creating a metallic object through weld-deposition in a layer by layer manner. Hence, they were limited in scope to single or limited multi-pass studies and the analysis of the behavior for weld-deposition was found lacking. The results presented here focused on the analysis of twin-wire weld-deposition for dissimilar materials. ER70S-6 and ER110S-G were the two wires selected for the same as they belonged to the same family of steels (hence, compatible for fusing together) with different hardness and tensile

properties. The results pertaining to their three combinations shown in next section for various values of torch speed and welding current have been presented here.

2 Materials and Methods

Gas metal arc welding of twin-wire deposition is comprised of two wires fitted into one torch. In twin-wire, controllable power sources can work individually with two separate filler wires feeding into a single weld pool. While the system synchronizes the frequency of the pulsing current to ensure a stable arc deposition, the current and the wire feed rate of each wire feeder can be independently controlled. Two trans plus synergic (TPS) weld-deposition unit's integration with the Robot machine has 6 axes, independent of its make. Stage of development is a key aspect in additive manufacturing. Weld deposition unit has to be integrated to robot in such a way that it should not affect the robot as well as interpolation as shown in Fig. 1. Copper coated ER 70S-6 (softer) and ER110S-G (harder) filler wires of diameter 1.2 mm were used for the experiments (Table 1). These two wires were divided into the following three cases, as shown in Fig. 2: Table 2 lists out the values of the parameters used for experiments.

1. Case-1: ER70S-6 + ER70S-6.
2. Case-2: ER110S-G + ER110S-G.
3. Case-3: ER110S-G + ER70S-6.

Deposition in single beads of length 120 mm each was carried out on a 28 mm thick MS plate (Base plate), shown in Fig. 3. The minimum current permissible was 70, 75 and 75 A for cases 1, 2 and 3 respectively. The maximum current was fixed at 250 A as the bead was too thick and

Fig. 1 Time twin-wire weld deposition setup



Table 1 Filler wires compositions

Elements	Ni	Al	Mn	Si	P	C
ER110S-6 in (%)	3.49	–	1.58	0.49	0.004	0.05
ER70S-6 in (%)	–	1.29	0.29	0.29	0.013	0.21

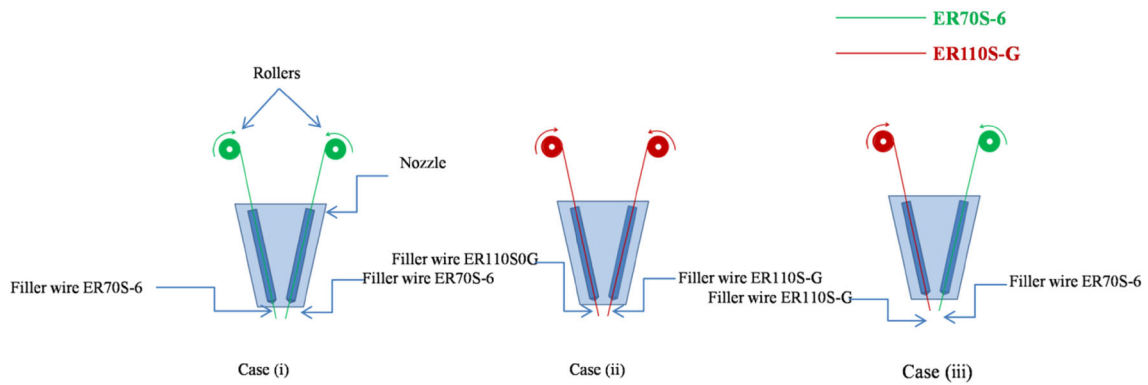


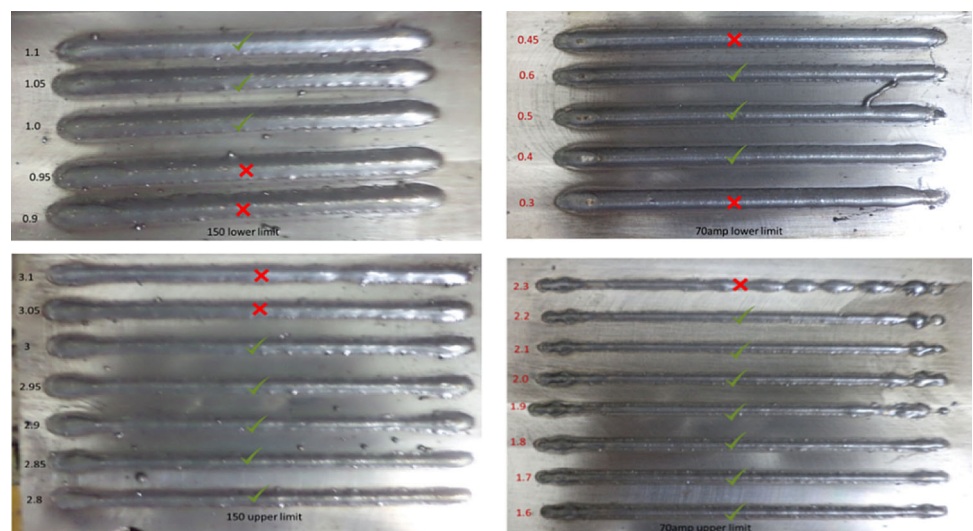
Fig. 2 The representation of the classification of filler wire

Table 2 Values of the parameters used for experiments

Parameter	Value
Nozzle gap (mm)	15
Torch speed (m/min)	0.1–5
Gas flow rare (l/min)	12
Filler wires dia (mm)	1.2
Wire speed (m/min)	2–5
Shielding gas	82% Ar + 18% CO ₂
Filler wires	ER110-G, ER70S-6

undesirable beyond that point. The current was varied in this range with increments of 5 A. The torch speed was increased from 0.1 to 5 m/min in increments of 0.1 m/min. The remaining process parameters were maintained at the constant values mentioned in Table 2. The feasible region of each combination was identified, as shown in Fig. 4. The shaded area in the figure was the overlapping region of all the three cases and hence, adopted as the working region as all the possible combinations were feasible here.

Fig. 3 Assortment of suitable weld profiles based on their continuity and bead geometry



3 Results and Discussion

3.1 Weld Bead Profile

To identify the parameters required to obtain a desired layer thickness or optimal step-over increment (distance between two passes during weld deposition), a geometry based model for predicting the weld bead properties based on current and torch speed used is very important. Literature suggests that the weld bead cross section follows a parabolic profile and that the optimal step-over increment is obtained when the step over increment is two-third of the weld bead width [5]. Experiments were carried out to confirm the suitability of this model for twin-wire deposition [7, 8]. As shown in the Fig. 5a, a set of nine various values of torch speed and current were chosen for each of combination of filler wires. The deposited weld beads of the same are shown in Fig. 5b–d.

The weld beads were sectioned with the help of a EDM machine and the boundary points on the same were measured with the help of a profile projector. Figure 6 shows

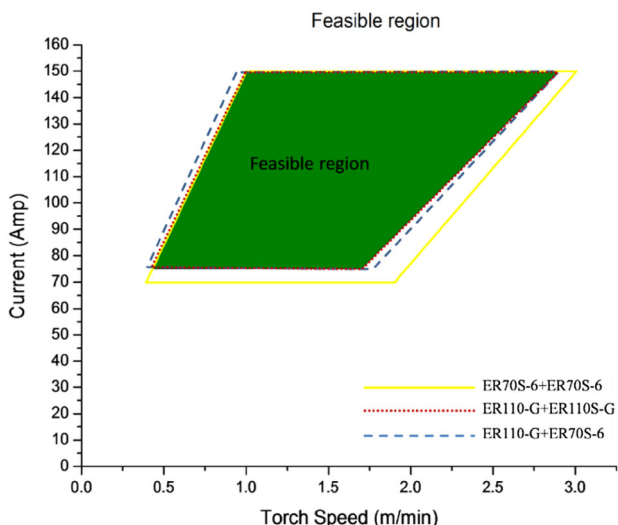


Fig. 4 Working range of various values of current and torch speed, and shaded area is feasible region with any combination of filler wires

one such cross section profile of a weld bead. The boundary points were then curve fitted to a symmetrical parabola and the geometrical parameters like width, height and area were calculated. Based on the parabolic assumption of the

weld bead, the area of the weld bead cross-section is given by,

$$A_m = \frac{2wh}{3}$$

where A_m area measured (mm^2); w weld bead width (mm); h weld bead height (mm).

The area of the weld bead cross-section could also be predicted based on the rate of filler wire coming out of the nozzle (wire speed, V_r) and the speed of the weld-deposition torch (torch speed, V_t). Thus, the predicted area of the weld bead is given by,

$$A_p = \frac{\pi d^2}{4V_t} [V_{r1} + V_{r2}]$$

where A_p area of bead predicted (mm^2); V_{r1} wire speed of filler wire 1 (ER70S-6 for cases-1 and 3, ER110S-G for case-2) (m/min); V_{r2} wire speed of filler wire 2 (ER70S-6 for case-1, ER110S-G for cases 2 and 3) (m/min); V_t torch speed in (m/min); d dia of filler wire (mm).

The measured and predicted weld bead geometries for these various cases have been listed in Tables 3, 4, 5; the same were plotted against a 45° line as shown in Fig. 7a–c. Interestingly, the error in case-3 was less than the other two

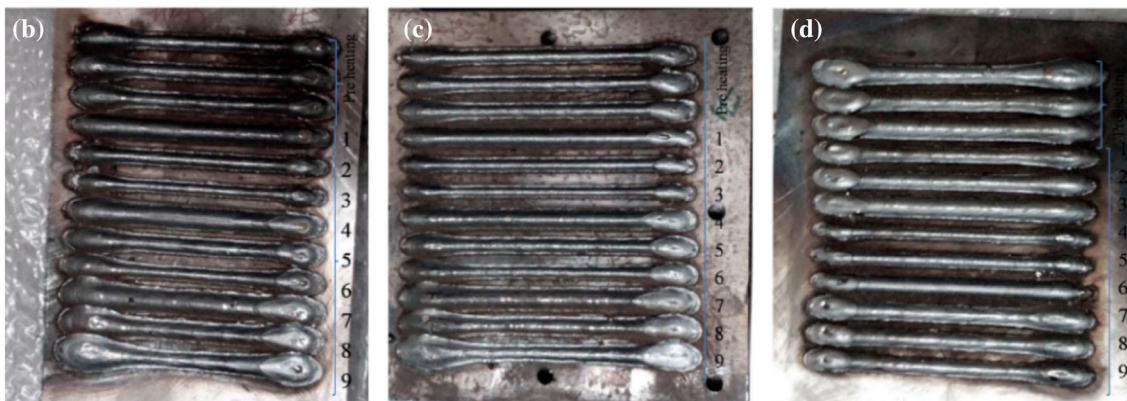
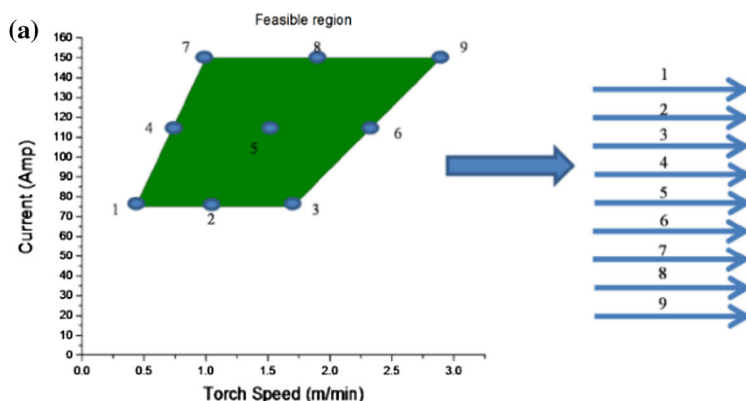


Fig. 5 Weld bead of boundary of each combination of filler wires after finding the feasibility of three combinations of wire. **a** Representation of boundary points and weld beads path of **b** ER70S-6 + ER70S-6, **c** ER110S-G + ER70S-6, **d** ER110S-G + ER110S-6

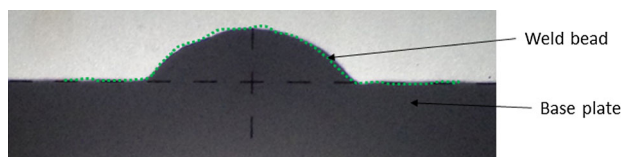


Fig. 6 Weld bead view while measuring using profile projector

cases, signaling a stable deposition even when dissimilar wires were used. The error in all the three cases was found to be under permissible limits. Hence, the parabolic assumption of weld bead cross section was adopted for the twin-wire welding. For optimal deposition, the step-over increment was 2/3rd of the weld bead width and the layer thickness equal to the weld bead height [5]. Second degree regression model was generated using observed experimental values, as shown below, for predicting bead height and width as a function of various values of torch and wire speed:

$$h = C_0 + C_1(v_{r1} + v_{r2}) + C_2v_t + C_3(v_{r1} + v_{r2})^2 + C_4v_t^2 + C_5v_t(v_{r1} + v_{r2})$$

$$w = C_0 + C_1(v_{r1} + v_{r2}) + C_2v_t + C_3(v_{r1} + v_{r2})^2 + C_4v_t^2 + C_5v_t(v_{r1} + v_{r2})$$

where, *h* height of weld bead in mm; *w* width of weld bead in mm.

*C*₀ – *C*₅ are the coefficient of regression model and corresponding values are listed in Table 6. The regression model was generated using LABFit software. The surface plot of the same is shown in Fig. 8.

3.1.1 Validation of Regression Model

To validate second degree regression model, four set of points from each combination of filler wire at arbitrary positions were selected. The experimentally measured weld

Table 3 Comparison of predicted and measured cross-sectional areas of the weld bead with twin-wire combination of ER70S-G + ER70S-G for various current and torch speed

S. no.	Weld parameters			Bead geometry				% Error
	Current (A)	Wire speed (<i>V_r</i> in m/min)	Torch speed (<i>V_t</i> in m/min)	Height (<i>h</i> in mm)	Width (<i>w</i> in mm)	Predicated area (in mm ²) $A = \frac{2\pi V_r d^2}{4V_t}$	Measured area (in mm ²) $A = \frac{2wh}{3}$	
1	75	2.10	0.50	2.14	6.12	9.50	8.73	-8.75
2	75	2.10	1.10	1.70	4.20	4.32	4.76	9.33
3	75	2.10	1.76	1.20	3.40	2.70	2.72	0.83
4	112	3.30	0.68	2.30	6.79	10.97	10.41	-5.38
5	112	3.30	1.49	1.78	4.41	5.01	5.23	4.32
6	112	3.30	2.29	1.35	3.41	3.26	3.07	-6.16
7	150	4.80	0.90	2.70	6.27	12.06	11.29	-6.84
8	150	4.80	1.90	1.49	5.32	5.71	5.28	-8.08
9	150	4.80	2.90	1.30	3.90	3.74	3.38	10.71

Table 4 Comparison of predicted and measured cross-sectional areas of the weld bead with twin-wire combination of ER110S-G + ER110S-G for various current and torch speed

S. no.	Weld parameters			Bead geometry				% Error
	Current (A)	Wire speed (<i>V_r</i> in m/min)	Torch speed (<i>V_t</i> in m/min)	Height (<i>h</i> in mm)	Width (<i>w</i> in mm)	Predicated area (in mm ²) $A = \frac{2\pi V_r d^2}{4V_t}$	Measured area (in mm ²) $A = \frac{2wh}{3}$	
1	75	2.0	0.50	2.30	6.10	9.04	9.35	3.32
2	75	2.0	1.10	1.40	4.20	4.11	3.92	4.86
3	75	2.0	1.70	1.20	3.50	2.66	2.80	5.01
4	112	3.1	0.69	2.30	6.60	10.16	10.12	-0.37
5	112	3.1	1.49	1.79	4.41	4.71	5.23	9.92
6	112	3.1	2.29	1.24	3.41	3.07	2.78	-9.78
7	150	4.3	0.90	2.38	6.20	10.81	9.87	-9.35
8	150	4.3	1.90	1.48	5.27	5.13	5.25	2.46
9	150	4.3	2.90	1.28	3.71	3.36	3.17	-5.34

Table 5 Comparison of predicted and measured cross-sectional areas of the weld bead with twin-wire combination of ER110S-G + ER70S-G for various current and torch speed

S. no.	Weld parameters			Bead geometry					% Error
	Current (A)	Wire speed (m/min)		Torch speed V_t (m/min)	Height (h in mm)	Width (w in mm)	Predicated area (in mm^2) $\frac{2\pi(V_{r1}+V_{r2})d^2}{4V_t}$	Measured area (in mm^2) $A = \frac{2wh}{3}$	
		V_{r2} ER110S-G	V_{r1} ER70S-G						
1	75	2.0	2.1	0.50	2.40	6.20	9.27	9.92	6.56
2	75	2.0	2.1	1.10	1.52	4.21	4.21	4.27	1.24
3	75	2.0	2.1	1.70	1.20	3.30	2.73	2.73	-3.27
4	112	3.1	3.3	0.69	2.39	6.50	10.48	10.36	-1.24
5	112	3.1	3.3	1.49	1.79	4.50	4.86	5.37	9.58
6	112	3.1	3.3	2.29	1.40	3.39	3.16	3.16	-2.57
7	150	4.3	4.8	0.90	2.70	6.15	11.43	11.07	-3.25
8	150	4.3	4.8	1.90	1.70	5.30	5.41	6.01	9.87
9	150	4.3	4.8	2.90	1.40	3.90	3.55	3.55	2.55

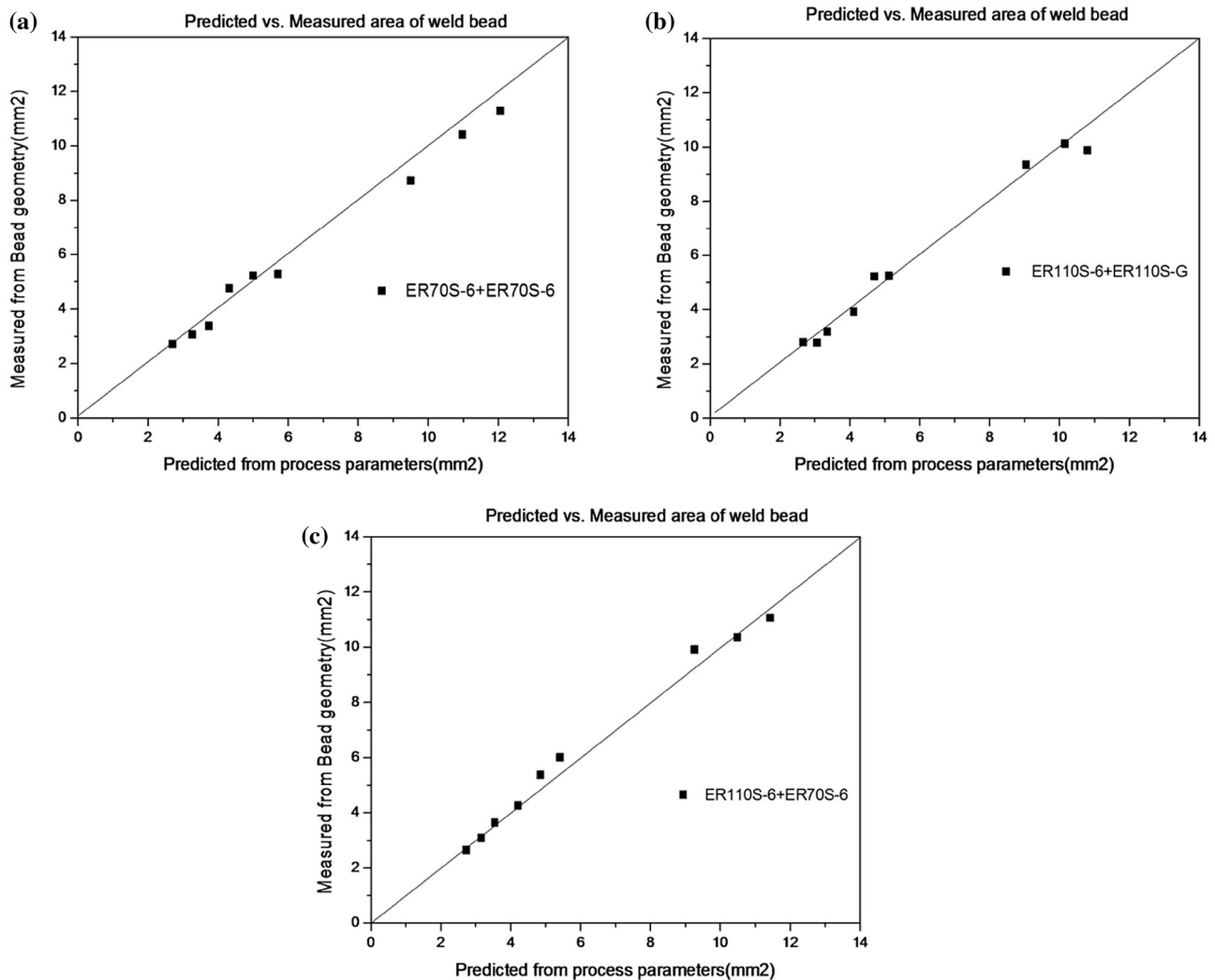
**Fig. 7** Predicted versus measured cross-sectional areas of the weld bead of three combination of filler wires, **a** ER70S-6 + ER70S-6, **b** ER110S-G + ER110S-G and **c** ER110S-G + ER70S-6

Table 6 Regression coefficient of area, width and height of weld beads for all combination of fillers

	ER70S-6 + ER70S-6		ER110S-G + ER110S-G		ER110S-G + ER70S-6	
	Width	Height	Width	Height	Width	Height
C ₀	5.44E+00	1.57E+00	5.57E+00	1.44E+00	5.84E+00	1.70E+00
C ₁	6.35E-01	3.07E-01	5.69E-01	4.57E-01	5.51E-01	3.63E-01
C ₂	-3.52E+00	-1.04E+00	-3.35E+00	-1.42E+00	-3.74E+00	-1.41E+00
C ₃	-3.43E-02	-4.30E-03	-3.27E-02	-2.34E-02	-3.90E-02	-1.09E-02
C ₄	2.82E-01	3.41E-01	1.72E-01	3.04E-01	1.08E-01	3.43E-01
C ₅	1.25E-01	-9.70E-02	1.62E-01	-3.16E-02	2.38E-01	-5.64E-02

bead geometry with bead width and height for these points were compared to the value predicted from regression model; these values are shown in Table 7. The maximum error was found to be 8.2%, indicating a good fit. The average correlation coefficient of the fit was 0.983776.

3.2 Effect of Deposition Parameters on Hardness

Twin-wire process is popular and well established for joining applications for which it has been primarily developed. The current research adapts the same process for metal deposition/cladding than just joining. However, as it is used for metal deposition of a layer in Additive Manufacturing, its context of application being different, the effect of deposition parameters have to be freshly looked into. The crucial difference between traditional welding and weld-deposition is the multiple (and numerous) number of passes and changing direction of the weld-deposition. Hence, the following considerations have been looked into:

1. Thermal steady-state condition
2. Torch direction
3. Number of overlapping beads

3.2.1 Thermal Steady-State Condition

Considerable amount of heat is generated during the weld-deposition process, which leads to the heating up of the base plate. Hence, the base plate temperature at the beginning is quite different from the temperature after a couple of weld-deposition passes. After a certain time, the heat added by weld-deposition equals the heat loss due to conduction and convection and further temperature change occurs in the base plate. The identification of this point helps in establishing the thermal steady-state condition thus enhancing the repeatability of the process.

Nine parallel weld-deposition beads of 120 mm each for each combination of filler wires were deposited on a plate of 160 mm × 160 mm × 10 mm at wire speed and torch speed values of 3.5 and 1.5 m/min respectively.

This set of experiments was repeated for three times as shown in Fig. 9a–i, to minimize error. These weld beads were cut cross sectionally and polished using emeries of grit size of 180, 360, 600, 1200, 1500, 2000 before the final diamond polish of 12μ, 6μ, and 1μ. They were then cleaned using ethanol solution. Subsequently, the micro-hardness of the cross-section of the weld beads were measured, as tabulated in Table 8. Figure 10 plots the hardness value of each bead with one presenting the first weld-bead (deposited on a base plate at room temperature) and the subsequent beads being deposited on the gradually heating base plate. As was inferred from the figure, the first three weld beads had high hardness values and it then gradually stabilized for the subsequent six beads. Hence, the thermal steady-state during experimentation (and a replication of the layered deposition scenario) could be achieved after the first three beads.

3.2.2 Effect of Torch Direction

In twin-wire, the direction of the weld-deposition has to be parallel to the filler wires, with one leading and the other trailing. As the leading and trailing wires can be dissimilar, the possible effect of this, if any, on the hardness of the weld-deposition was studied. Experiments were conducted for different torch direction with different wire speeds viz. forward, backward direction. Figure 11 shows the representations of direction, wire speed and Fig. 12 shows the weld beads as deposited in the forward and backward direction. From the last section, it was found that thermal steady-state could be achieved after the first three beads. Considering that, of nine beads, first three beads were deposited for pre-heating and steady-state condition while of the remaining six beads, three beads were deposited in forward and three in the backward direction. The measured hardness values are listed in Table 9 and Fig. 13. As was inferred from Fig. 13, the torch direction did not have any effect on the hardness of the weld-deposition.

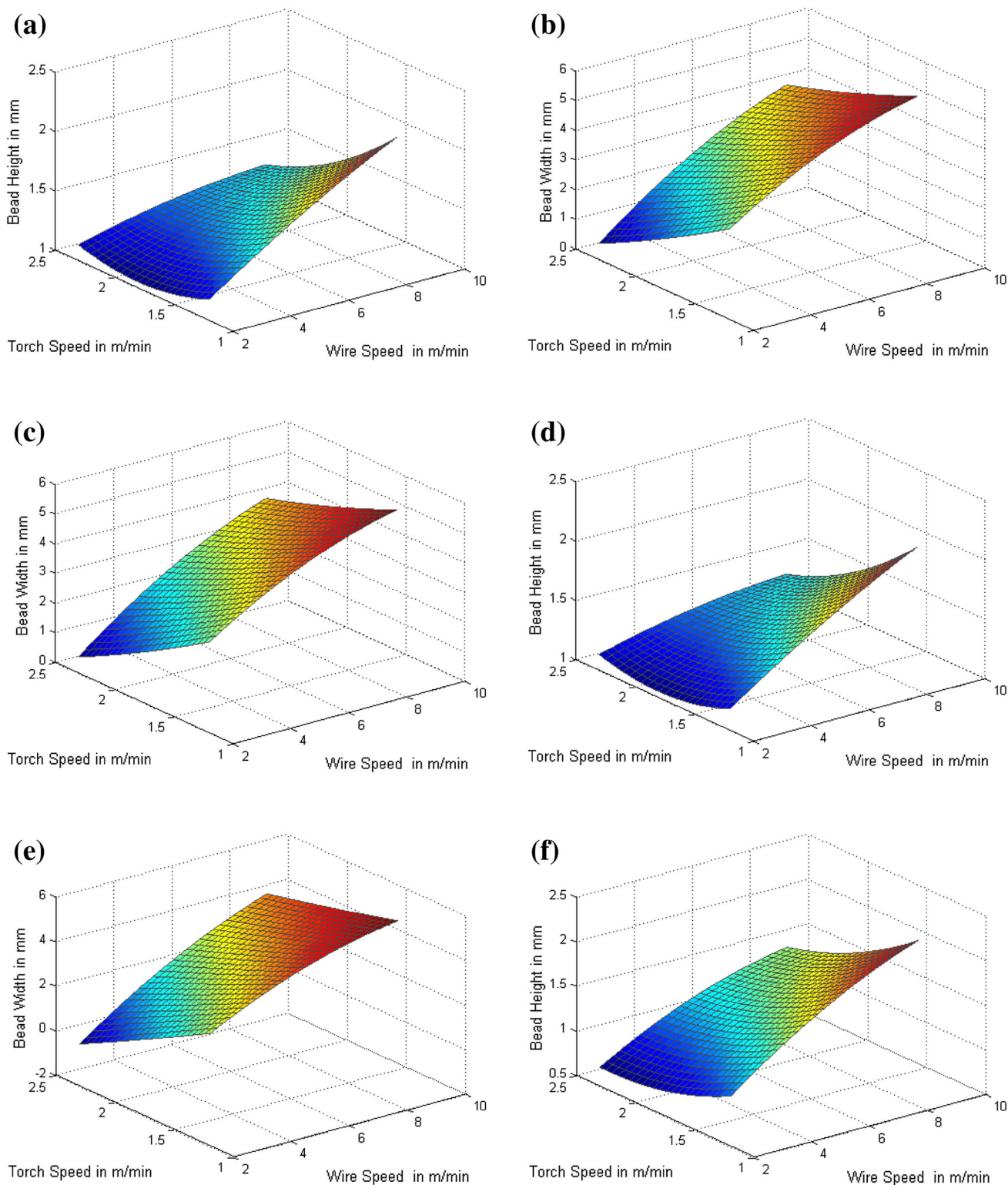


Fig. 8 Surface plots of weld bead shapes **a, b** ER70S-6 + ER70S-6, **c, d** ER110S-G + ER110S-G, **e, f** ER110S-G + ER70S-6

3.2.3 Effect of Bead Overlap

One important differentiating factor of weld-deposition from other forms of welding is that weld beads partially

overlap with each other. This results in a deposited weld-bead being subjected to another phase of heating and partial-remelting when the next weld-deposition pass is made. Based on the feature size of the layer being

Table 7 Weld bead geometry for validation points

S. no.	Filler wire combination	Current I (A)	Wire speed (m/min)		Torch speed V_t (m/min)	Bead geometry (mm)					
			V_{r1}	V_{r2}		Measured experimentally		Predicted from regression fit		Error (%)	
						Width w	Height h	Width w	Height h	Width	Height
1	ER70S-6 + ER70S-6	90	2.6	2.6	0.54	6.12	2.20	6.35	2.32	-3.70	-5.24
2		90	2.6	2.6	1.94	3.40	1.30	3.30	1.34	2.90	-2.73
3		120	3.5	3.5	0.77	6.34	2.40	6.33	2.39	0.12	0.60
4		120	3.5	3.5	2.42	3.40	1.24	3.44	1.34	-1.31	-8.20
5	ER110S-G + ER110S-G	90	2.5	2.5	0.54	6.10	2.20	6.28	2.27	-2.88	-3.33
6		90	2.5	2.5	1.94	3.40	1.30	3.20	1.32	6.00	-1.58
7		120	3.4	3.4	0.77	6.10	2.40	6.28	2.35	-2.97	2.03
8		120	3.4	3.4	2.42	3.40	1.36	3.35	1.34	1.41	1.53
9	ER110S-G + ER70S-6	90	2.5	2.6	0.54	6.30	2.27	6.31	2.29	-0.18	-1.07
10		90	2.5	2.6	1.94	3.10	1.40	3.25	1.33	-4.81	5.14
11		120	3.4	3.5	0.77	6.18	2.32	6.31	2.37	-2.06	-2.09
12		120	3.4	3.5	2.42	3.60	1.40	3.40	1.34	5.59	4.25

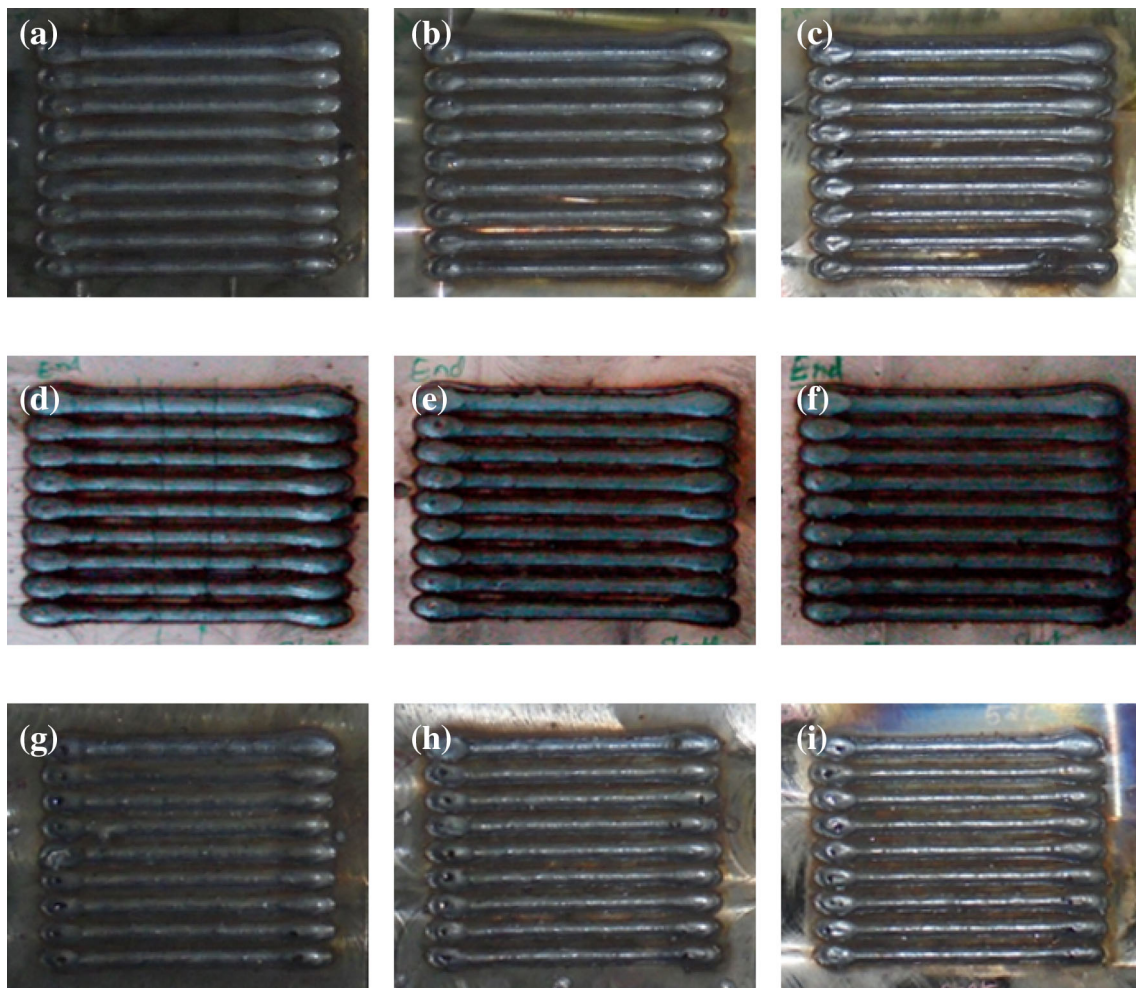


Fig. 9 Identifying steady state condition of hardness values **a–c** ER70S-6 + ER70S-6, **d–f** ER110S-G + ER110S-G, **g–i** ER110S-G + ER70S-6

Table 8 Hardness values of steady state condition for three combination of two filler wires

S. no.	Wire speed in m/min		Weld bead order no	Hardness values in HV		
	Nozzle-1	Nozzle-2		ER70S-6 + ER70S-6	ER110S-G + ER110S-G	ER110S-G + ER70S-6
1	3.5	3.5	1	404.33	495.00	452.00
2	3.5	3.5	2	380.00	485.73	430.00
3	3.5	3.5	3	370.00	484.33	425.00
4	3.5	3.5	4	358.73	481.13	418.00
5	3.5	3.5	5	345.27	473.13	420.00
6	3.5	3.5	6	350.00	471.93	422.00
7	3.5	3.5	7	355.00	475.00	418.00
8	3.5	3.5	8	349.00	479.00	417.00
9	3.5	3.5	9	352.00	481.00	421.00

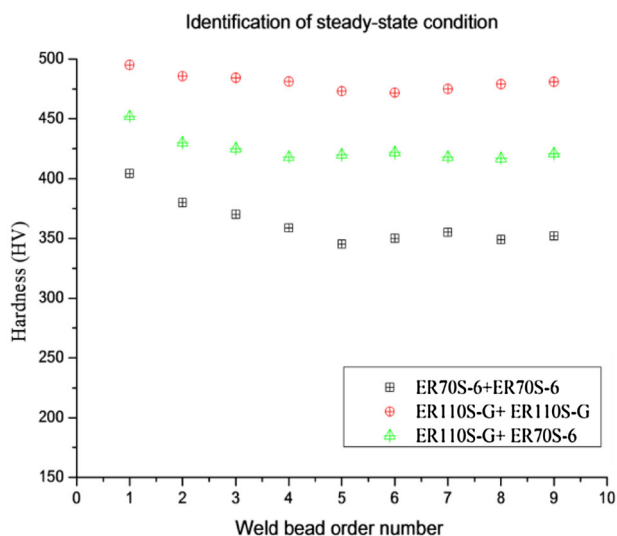
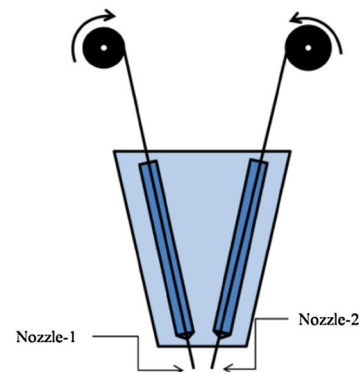
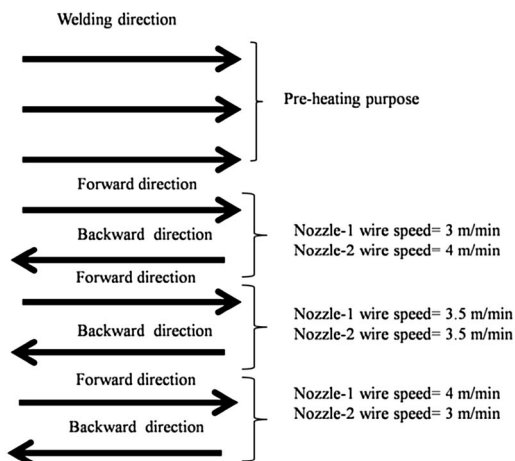


Fig. 10 Hardness values of deposited weld bead for identification of steady-state condition

deposited, the number of passes to be made may also change; a thin wall for example may need only two passes while a thicker wall may require four passes.

Fig. 11 Schematic representation of weld torch direction and wire speed



Hence, a set of experiments were conducted to find the effect of overlapping weld beads. Figure 14 shows the deposited overlapping two, three and five weld beads for three combinations of fillers, with a stepover increment of 3 mm. The measured values are listed in Table 10 and the corresponding values are plotted in Fig. 15. From the figure, it was clear that, as a result of partial remelting, the overlapping beads had less hardness compared to single bead. After three beads, the hardness stabilized and did not change much. It might be noted that single beads deposition would have higher hardness than overlapping beads and hence must be avoided during area-filling of a given layer. However, as most of the weld deposition in a layer demand multiple passes, the deposition process will not be a severe constraint.

4 Conclusion

The capability of twin-wire based weld-deposition for obtaining functionally gradient objects through use of a combination of different filler wires have been illustrated.

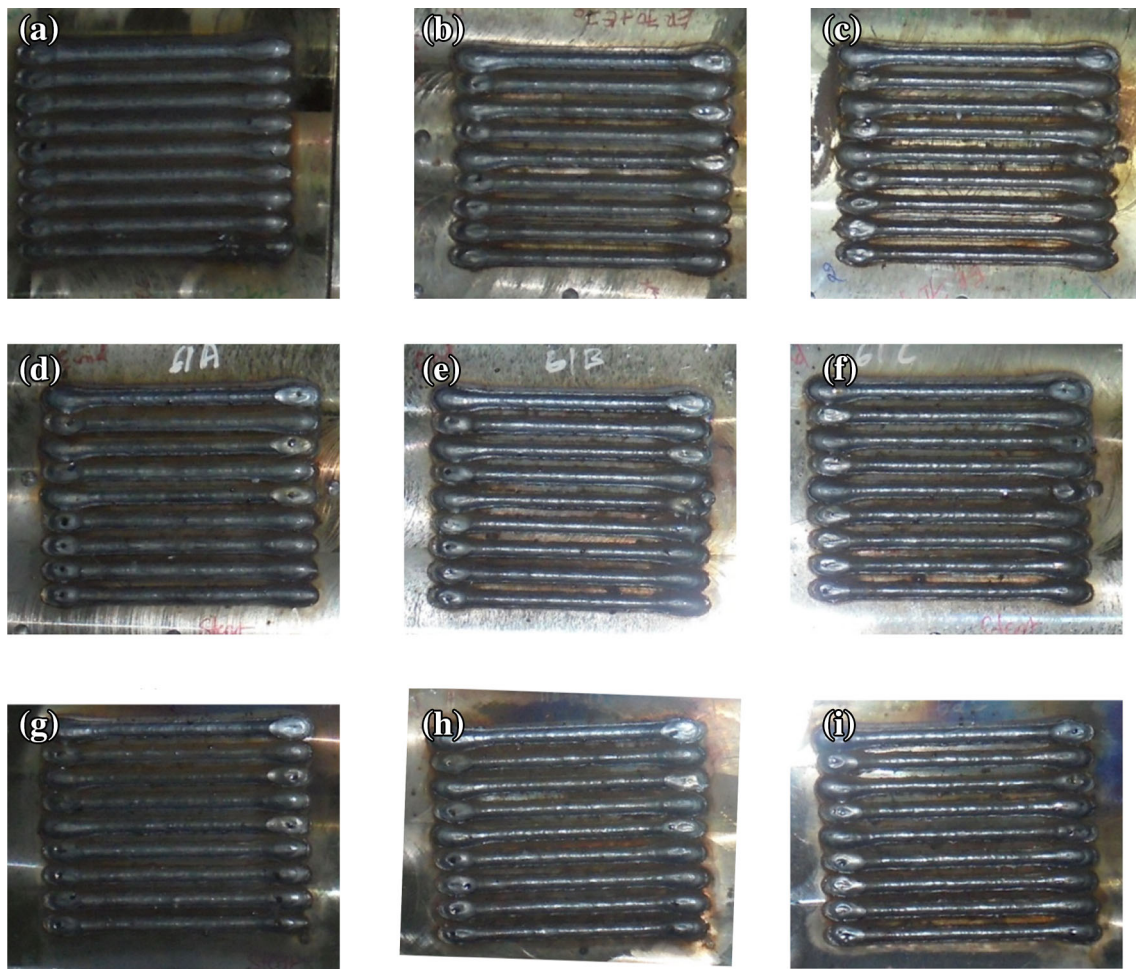


Fig. 12 Weld bead deposited in two directions **a–c** ER70S-6 + ER70S-6, **d–f** ER110S-G + ER110S-G, **g–i** ER110S-G + ER70S-6

Table 9 Hardness values of different torch direction

S. no.	Wire speed in m/min		Torch direction	Bead order no	Hardness values in HV		
	Nozzle-1	Nozzle-2			ER70S-6 + ER70S-6	ER110S-G + ER110S-G	ER110S-G + ER70S-6
1	3	4	Forward	4	351.00	479.00	420.00
2	3	4	Backward	5	352.00	473.00	419.00
3	3.5	3.5	Forward	6	355.00	475.00	420.00
4	3.5	3.5	Backward	7	351.00	471.00	422.00
5	4	3	Forward	8	351.00	468.00	420.00
6	4	4	Backward	9	354.00	472.00	419.00

Two filler wires viz., ER70S-6 and ER110S-G, the former having lower hardness than the latter, were used for the experimentation. The operating range of the process parameters viz., current and torch speed for the three possible combinations of the filler wires were determined and the feasible working region was obtained from the same.

Earlier work on weld bead cross section suggested that it followed a parabolic profile with the optimal step-over increment being two-third of the weld bead width. Experimental investigation of the weld-bead cross section for various values of wire and torch speeds confirmed the suitability of this model for twin-wire deposition. A second degree regression model was also computed for predicting

Fig. 13 Effect of different torch direction

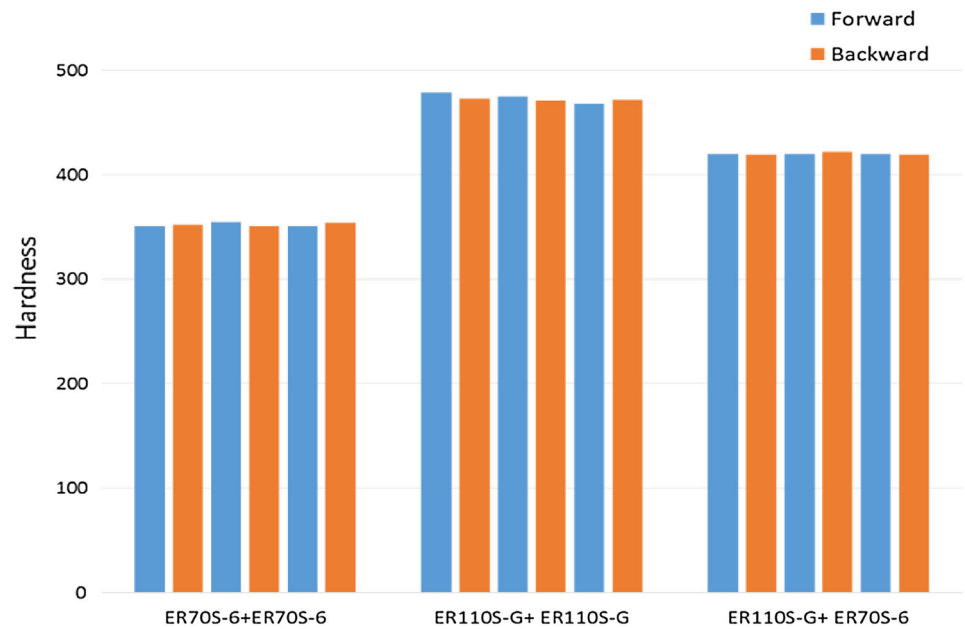


Fig. 14 The weld beads of **a** two overlap beads, **b** three overlap beads, **c** five overlap beads

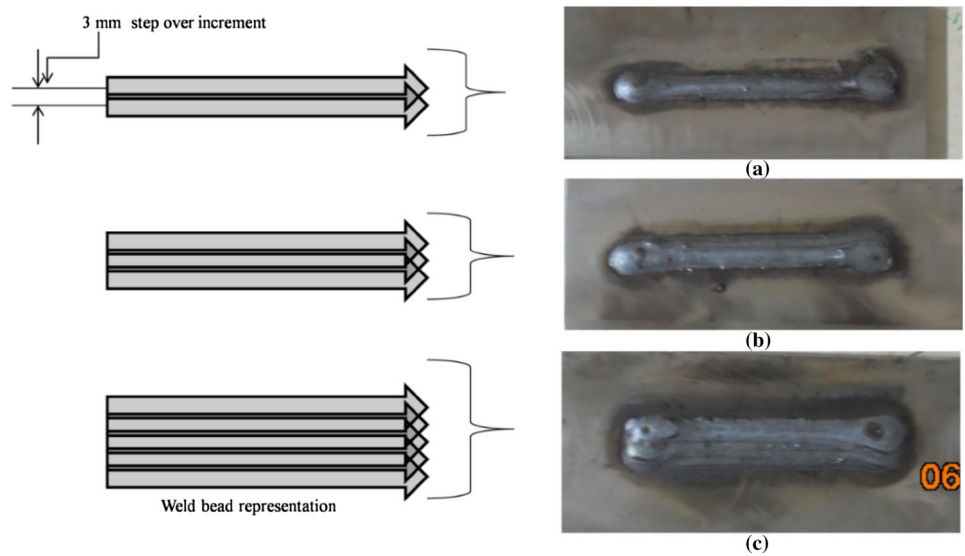


Table 10 Hardness values of single and overlap beads

S. no.	Wire speed in m/min		Average hardness values in HV			
	Nozzle-1	Nozzle-2	Single bead	Two beads	Three beads	Five beads
1	3.5	3.5	440.00	300.00	255.00	248.80
2	3.5	3.5	450.00	294.00	249.33	250.60
3	3.5	3.5	450.00	301.00	248.00	249.20
4	3.5	3.5	446.00	292.50	249.67	249.20
5	3.5	3.5	453.00	295.50	251.33	250.80
6	3.5	3.5	452.00	286.50	250.67	248.60

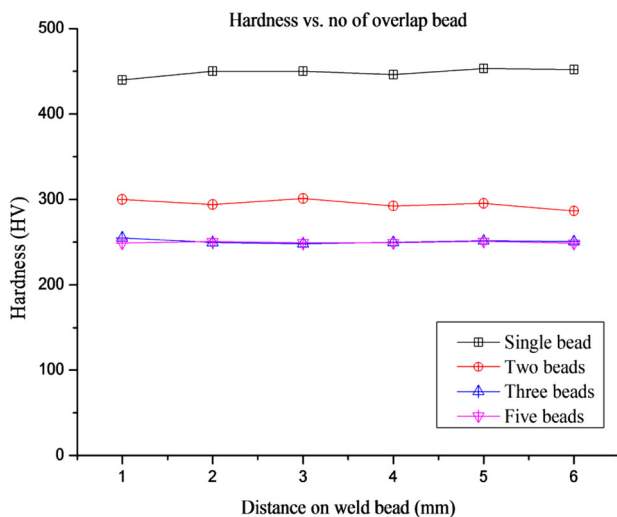


Fig. 15 Effect of hardness on number of beads deposited for filler wire combination (ER110S-G + ER70S-6)

weld bead width and height as a function of wire speed and torch speed. Subsequently, model was validated and the maximum error was found to be 8.2%, indicating a good fit and thus validating the regression model.

Criterion for adopting the twin-wire process from joining to metal deposition/cladding was also studied. It was found that during weld-deposition of multiple passes, thermal steady state reached after three weld-beads. Although in dissimilar twin-wire welding, the leading and trailing wires might be different for forward and backward torch direction, it was found that the torch direction did not have any effect on the hardness of the weld-dead deposited. However, the number of overlap beads was observed to have an effect on the hardness with single beads having higher hardness than overlapping multiple beads. This was due to another phase of heating and partial-remelting took place when the next weld-deposition pass was made.

Acknowledgements The authors gratefully acknowledge the partial funding support received from the Department of Science and Technology, Government of India.

References

1. Spencer J D, Dickens P M, and Wykes C M, *Proc Inst Mech Eng Part B J Eng Manuf* **212** (1998) 175.
2. Song Y-A, and Park S J, *Mater Process Technol* **171** (2006) 35.
3. Akula S, and Karunakaran K P, *Robot Comput Integr Manuf* **22** (2006) 113.
4. Karunakaran K P, Suryakumar S, Pushpa V, and Akula S, *Robot Comput Integr Manuf* **26** (2010) 490.
5. Suryakumar S, Karunakaran K P, Bernard A, Chandrasekhar U, Raghavender N, and Sharma D, *Comput Des* **43** (2011) 331.
6. Suryakumar S, Karunakaran K, Chandrasekhar U, and Somashekara M, *Proc Inst Mech Eng Part B J Eng Manuf* **227** (2013) 1138.
7. Suryakumar S, and Somashekara M A, in *24th International SFF Symposium—An Additive Manufacturing Conference, SFF 2013*, University of Texas at Austin (freeform) (2013), p 939.
8. Adinarayanappa S M, and Simhambhatla S, in *19th Design for Manufacturing and the Life Cycle Conference. 8th International Conference Micro-Nanosystem*, Vol. 4. ASME (2014), p V004T06A003.
9. Gao M, Mei S, Wang Z, Li X, and Zeng X, *J Mater Process Technol* **212** (2012) 1338.
10. Pal K, and Pal S K, *CIRP J Manuf Sci Technol* **3** (2010) 55.
11. Zhang H T, Feng J C, He P, and Hackl H, *Mater Charact* **58** (2007) 588.
12. Zhang H, and Liu J, *Mater Sci Eng A* **528** (2011) 6179.
13. Qin G, Su Y, and Wang S, *Trans Nonferrous Metals Soc China* **24** (2014) 989.
14. Gulenc B, Develi K, Kahraman N, and Durgutlu A, *Int J Hydrogen Energy* **30** (2005) 1475.
15. Yan J, Zeng X, Gao M, Lai J, and Lin T, *Appl Surf Sci* **255** (2009) 7307.
16. Fang C, Meng X, Hu Q, Wang F, Ren H, Wang H, Guo Y, and Mao M, *J Iron Steel Res Int* **19** (2012) 79.
17. Ruan Y, Qiu X M, Gong W B, Sun D Q, and Li Y P, *Mater Des* **35** (2012) 20.
18. Lin J, Wang Z, Lin P, Cheng J, Zhang X, and Hong S, *Surf Coatings Technol* **240** (2014) 432.
19. Tušek J, *J Mater Process Technol* **100** (2000) 250.
20. Meng Q G, Fang H Y, Yang J G, and Ji S D, *Theor Appl Fract Mech* **44** (2005) 178.
21. Yang X, Xu Q, Yin N, and Xiao X, *J Wuhan Univ Technol Sci Ed* **26** (2011) 114.